The Molecular Anatomy of a Calcium-Binding Protein

STURE FORSÉN* AND JOHAN KÖRDEL

Department of Physical Chemistry 2, University of Lund, P.O. Box 124, S-221 00 Lund, Sweden

THOMAS GRUNDSTRÖM

Unit of Applied Cell and Molecular Biology, University of Umeå, S-901 87 Umeå, Sweden

WALTER J. CHAZIN

Department of Molecular Biology, The Scripps Research Institute, La Jolla, California 92037

Received April 1, 1992

Calcium ions (Ca^{2+}) play an important role as a signal or messenger in a wide variety of cellular processes including metabolism, cell division and growth, secretion, ion transport, and muscle contraction. The signal or message involves changes in the concentration of calcium that are interpreted by a family of structurally homologous Ca^{2+}-binding proteins. For example, calmodulin (CaM) and troponin C (TnC) are regulatory proteins that respond to transitory increases in intracellular Ca^{2+} concentration by undergoing Ca^{2+}-dependent conformational changes, which in turn alter their interactions with target proteins and lead to specific cellular responses. X-ray crystallographic studies have been carried out on the Ca^{2+} loaded forms of six members of this family of proteins,[1-7] and it has been found that they share a common helix–loop–helix structural motif in their Ca^{2+}-binding sites, termed the "EF-hand"[8] or the "calmodulin fold".[9] A second feature of this family of proteins is that pairs of helix–loop–helix binding sites rather than individual sites seem to be the functional unit.[10] The pairwise parallel arrangement of sites appears to lead to increased Ca^{2+} affinity over that of an isolated helix–loop–helix binding site and provides a likely mechanism for cooperative Ca^{2+} binding, involving the cross-strand hydrogen bonds between the two Ca^{2+}-binding loops.[11-13] The positive cooperativity observed in EF-hand Ca^{2+}-binding proteins very likely plays an important role in Nature, since it allows cellular events to be regulated by modest changes in intracellular Ca^{2+} concentrations.

Our present knowledge of the detailed molecular mechanisms behind the function and specific properties of proteins of the EF-hand Ca^{2+}-binding proteins is, however, very limited. Although both CaM (M_r 16 700; four Ca^{2+}-binding sites) and TnC (M_r 18 000; four Ca^{2+} sites) are of utmost biological interest, the complications associated with the presence of four Ca^{2+}-binding sites make their binding properties extremely difficult to study by present-day methods for detailed structure–function studies. For example, it is difficult to measure four fairly similar binding constants accurately and to disentangle the kinetic scheme for the dissociation of four Ca^{2+} ions. As an initial step toward comprehensive studies of structure–function relations of EF-hand Ca^{2+}-binding proteins we have undertaken studies of bovine calbindin D_{9k} (M_r 8500; two Ca^{2+} sites). The structure of the protein (Figure 1) strongly resembles that of the globular domains of CaM and TnC.[14] Its small size makes it well suited for detailed biophysical studies, in particular structural analysis by two-dimensional (2D) ^1H nuclear magnetic resonance (NMR) spectroscopy.

Our studies of calbindin D_{9k} are based on utilizing the powerful combination of biophysical techniques and site-directed mutagenesis. The major issues of interest include (i) the molecular basis for the high affinity, specificity, and cooperativity in metal ion binding, with

Sture Forsén was born in Piteå, Sweden, in 1932. He received a Ph.D. from the Royal Institute of Technology in Stockholm and was appointed Professor of Physical Chemistry 1963–1967. Since 1966 he has held a chair in Physical Chemistry at the University of Lund. In the mid-1970s his NMR work on quadrupolar nuclei brought him in contact with biochemical problems such as structure–function studies of proteins, which have developed into his primary area of research.

Johan Kördel was born in Norrköping, Sweden, in 1962 and obtained his Ph.D. from the University of Lund, under the joint supervision of Sture Forsén and Walter J. Chazin. He is presently a postdoctoral fellow with Gerhard Wagner at Harvard Medical School, Boston.

Thomas Grundström was born in Skellefteå, Sweden, in 1953. He obtained his Ph.D. from the University of Umeå with Staffan Normark. After 2 years of postdoctoral study with Pierre Chambon in Strasbourg, France, he was appointed Assistant Professor of Molecular Biology at the University of Umeå in 1984. His research interests include the structure and function of transcription factors and calcium-binding proteins.

Walter J. Chazin was born in Lackawanna, New York, in 1954. He obtained his Ph.D. from Concordia University (Montréal) with L. D. Colebrook. After postdoctoral training with Kurt Wüthrich (E.T.H., Zürich) and Peter E. Wright (Scripps Research Institute), he was appointed Assistant (1987) and then Associate (1992) Professor of Molecular Biology. His research interests are in NMR studies of the structure and dynamics of proteins and oligonucleotides.

(1) Moews, P. C.; Kretsinger, R. H. *J. Mol. Biol.* **1975**, *91*, 201–228.
(2) Szebenyi, D. M. E.; Moffat, K. *J. Biol. Chem.* **1986**, *261*, 8761–8777.
(3) Babu, Y. S.; Bugg, C. E.; Cook, W. J. *J. Mol. Biol.* **1988**, *204*, 191–204.
(4) Herzberg, O.; James, M. N. G. *J. Mol. Biol.* **1989**, *261*, 2638–2644.
(5) Satyshur, K. A.; Sambhorao, T. R.; Pyzalska, D.; Drendall, W.; Greaser, M.; Sundaralingam, M. *J. Biol. Chem.* **1988**, *263*, 1628–1647.
(6) Ahmed, F. R.; Przybylska, M.; Rose, D. R.; Birnbaum, G. I.; Pippy, M. E.; MacManus, J. P. *J. Mol. Biol.* **1990**, *216*, 127–140.
(7) Cook, W. J.; Ealick, S. E.; Babu, Y. S.; Cox, J. A.; Vijay-Kumar, S. *J. Mol. Biol.* **1991**, *266*, 652–656.
(8) Kretsinger, R. H. *Nature (London)* **1972**, *240*, 85–88.
(9) Kretsinger, R. H. *Cold Spring Harbor Symp. Quant. Biol.* **1987**, *52*, 499–510.
(10) Seamon, K. B.; Kretsinger, R. H. *Met. Ions Biol.* **1983**, *6*, 1–51.
(11) Forsén, S.; Vogel, H.; Drakenberg, T. *Calcium and Cell Function*; Cheung, W. Y., Ed.; Academic Press: New York, 1986; Vol. 6, pp 113–157.
(12) Linse, S.; Brodin, P.; Drakenberg, T.; Thulin, E.; Sellers, P.; Elmdén, K.; Grundström, T.; Forsén, S. *Biochemistry* **1987**, *26*, 6723–6735.
(13) Williams, T. C.; Corson, D. C.; Sykes, B. D.; MacManus, J. P. *J. Biol. Chem.* **1987**, *262*, 6248–6256.
(14) Strynadka, N. C. J.; James, M. N. G. *Annu. Rev. Biochem.* **1989**, *58*, 951–998.

0001-4842/93/0126-0007$04.00/0

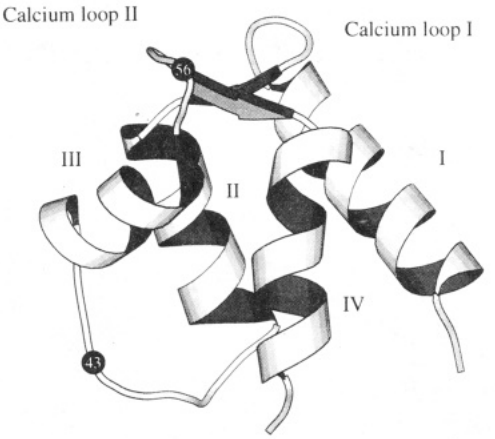

Figure 1. Ribbon diagram of calbindin D_{9k}. The coordinates of the average solution structure of calcium-loaded P43G calbindin D_{9k}[33] were used to generate this schematic diagram. The coils represent helices (numbered I–IV) and the arrows the short β-type interaction. The position of residues 43 and 56 are indicated by their residue numbers. The figure was produced with the program MOLSCRIPT.[58]

particular emphasis to date on the role of short-range and long-range electrostatic interactions, (ii) the structural rearrangements and changes in dynamic properties that accompany Ca^{2+} binding, and (iii) the interactions that determine the stability of calbindin D_{9k} toward unfolding. Although our main aim is to gain insight into the structure–function relationships in this specific family of proteins, it is obvious that some of the results we have obtained are of relevance to proteins in general.

Gene Synthesis and Expression

To produce bovine calbindin D_{9k} in *Escherichia coli*, a gene was designed encoding the known amino acid sequence of the protein.[15] A codon selection that mimics that in highly expressed *E. coli* genes was chosen. The wild-type gene was constructed from "DNA building blocks", sets of overlapping oligonucleotides bordered by restriction enzyme sites. Genes for calbindin D_{9k} mutants were constructed by reassembly of the DNA segment containing the substitution(s) desired. To facilitate the construction of mutations, DNA segments corresponding to different parts of the protein were replaced by polylinkers. Thereby complete mutated genes could be assembled in one step, using a small set of oligonucleotides with replacement of those containing the codons to be changed.

A critical factor for advanced biophysical analysis of a protein, in particular for NMR, is expression of sufficiently high amounts. To achieve efficient transcription and translation of calbindin D_{9k}, we used the strongly inducible tac promoter, controlled by the lacIq repressor, and an optimized ribosome binding sequence at the start codon. Initially a high copy number plasmid, pICB1, was used to establish high gene dosage.[15] Later the expression level was further improved by the use of a plasmid with temperature-sensitive replication control, pRCB1.[16] When the temperature is raised above 35 °C, the number of copies per cell of this plasmid increases continuously, thereby increasing the gene dosage of the calbindin D_{9k} gene. The optimized level of expression of calbindin D_{9k} reached as much as 10% (w/w) of total *E. coli* protein, which due to the low molecular weight is many-fold higher in molar terms. This high expression level enables production of isotopically labeled protein in sufficient quantities for NMR analysis at an affordable cost.[17] For example, the production of calbindin D_{9k} with all but a selected number of amino acids fully deuterated was achieved by growing the bacterium in a minimal salt medium in D_2O with deuterated algal hydrolysate and the selected protonated amino acid(s).[16]

Physical Characterization

The initial preparations of recombinant calbindin D_{9k} were characterized by SDS-PAGE and agarose gel electrophoresis, amino acid composition, partial or complete amino acid sequencing, and ^1H NMR spectroscopy. By these methods each sample appears as a homogeneous preparation. However, when these samples are examined by 2D ^1H NMR spectroscopy, a large excess of cross peaks is observed in nearly all regions of the spectra. This prompted more in-depth characterization of purity by gel electrophoresis, and using isoelectric focusing (IEF) it was clearly evident that preparations previously regarded as homogeneous were in fact mixtures of isoforms.[18] Differences in the rates of migration on IEF gels indicate that the various isoforms differ in net charge. To identify the molecular basis of these isoforms, they were separated by chromatographic methods and further characterized by protein sequencing and 2D ^1H NMR. In fact, two nonnative forms of the protein were identified, both byproducts of deamidation of Asn56 in calcium-loop II. A detailed analysis by 2D ^1H NMR of the mixture of nonnative isoforms provided complete sequential ^1H resonance assignments for both species and sufficient information to establish that these two species correspond to the α- and β-linked products of deamidation.[18] Once identified, the generation of deamidated protein could be controlled by substituting a heat-denaturation step for the standard urea denaturation step in the purification procedure.

To verify that the non-deamidated preparations were fully homogeneous, 2D ^1H NMR spectra were acquired for the purified protein. To our surprise, there was still a large excess of cross peaks in all spectral regions, with rather clear evidence of two species in a 3:1 ratio in solution. On the basis of the extensive biochemical evidence of the chemically homogeneity of the sample, this indicated that the native protein must be *conformationally* heterogeneous. 2D ^1H NMR chemical exchange experiments provided direct evidence that the two species in solution are in equilibrium. To gain insight into the specific cause of this conformational heterogeneity, it was necessary to obtain complete sequence-specific ^1H NMR assignments for both the major and minor isoforms simultaneously. This provided a residue-by-residue comparison of the chemical shifts of the major and minor conformational isomers,

(15) Brodin, P.; Grundström, T.; Hofmann, T.; Drakenberg, T.; Thulin, E.; Forsén, S. *Biochemistry* **1986**, *25*, 5371–5377.

(16) Brodin, P.; Drakenberg, T.; Thulin, E.; Forsén, S.; Grundström, T. *Protein Eng.* **1989**, *2*, 353–358.

(17) Skelton, N. J.; Akke, M.; Kördel, J.; Thulin, E.; Forsén, S.; Chazin, W. J. *FEBS Lett.* **1992**, *303*, 136–140.

(18) Chazin, W. J.; Kördel, J.; Drakenberg, T.; Thulin, E.; Hofmann, T.; Forsén, S. *Biochemistry* **1989**, *28*, 8646–8653.

which implicated structural differences in the polypeptide segment Ser38–Asp54. The most likely candidate for the physical process leading to conformational heterogeneity was cis–trans isomerization of Pro43. Using nuclear Overhauser effects (NOEs) that can unambiguously define the conformation of a proline peptide bond,[19] it was possible to establish unambiguously that the major species corresponds to protein with a *trans*-Gly42–Pro43 peptide bond and that the minor species corresponds to the *cis*-Pro43 isomer.[20] Two isoforms are also observed in a similar ratio in the apo state of calbindin D_{9k}. Prompted by these findings, in the recent 1.6-Å crystal structure of calcium-loaded calbindin D_{9k} two conformations are occupied by residues Lys41–Pro43, corresponding to the *trans*-Pro43 and *cis*-Pro43 isomers, in order to obtain a better fit to the electron density map in this region.[21]

The direct and sequence-specific identification of the isopeptide bond and of the two isoforms in chemical equilibrium due to proline cis–trans isomerism are novel applications of ^{1}H NMR for the study of protein structure. We believe that the occurrence of these phenomena is more widespread than is commonly recognized and that, with the technological and methodological advancement of structural biology, observations of this kind will become more commonplace.

Consequences of Calcium Binding on Structure and Dynamics

The principal long-term objective of structural research on the calmodulin superfamily of calcium-binding proteins is to identify the role of molecular conformation and dynamics in determining protein function and metal ion specificity. To fully understand the structural and dynamical consequences of Ca^{2+} binding, specific binding domains must be examined in both the inactive (apo or Mg^{2+}-bound) and Ca^{2+}-activated states. Since it has not been possible to crystallize any members of this family of proteins with different levels of Ca^{2+} occupancy in a specific domain, the method of three-dimensional structure determination using NMR spectroscopy in solution is uniquely suited to this problem. This technique is being applied to obtain in-depth information on the structure and dynamics of calbindin D_{9k}, with an initial emphasis on generating high-resolution solution structures of the apo and Ca^{2+}-loaded states.

The initial work on the calcium-loaded protein, including sequence-specific assignments, analysis of the elements of secondary structure, and determination of the global folding pattern, was carried out on the native protein from porcine intestine[22] and the wild-type minor A form of the bovine protein expressed in *E. coli*.[23,24] From these data, we were able to carry out a comparative analysis of the major and minor species of the wild-type protein, as well as make further comparisons to a mutant protein in which the conformationally heterogeneous Pro43 residue was substituted by glycine.[24] The comparative studies were important in establishing that the P43G mutant protein could be substituted for the wild-type protein to simplify the spectroscopic analysis for structure determination. However, calculations of the three-dimensional solution structure were first carried out on the native porcine protein in the calcium-loaded state to validate the study of recombinant minor A sequence as opposed to the full-length sequence.[25] A close correspondence is found between the structures of the intact porcine protein and the minor A form of the bovine protein.

The primary ^{1}H NMR analysis of the apo states of both the wild-type and P43G proteins has been completed.[26] The results from these studies allowed a thorough characterization of the elements of secondary structure and the global folding pattern an together with previous studies provided a first level of comparison of the structure and dynamics of the calcium-free and calcium-bound states of the protein. This analysis revealed that although there are widespread and very significant changes in chemical shifts throughout the protein in response to binding of calcium, there are virtually no changes in the sequential NOEs, backbone NH–C$^\alpha$H scalar couplings, the derived elements of secondary structure, and the global folding pattern.[27] The tertiary structures are, at least, very similar. In contrast, measurements of the backbone amide proton exchange rates and the aromatic ring flip rates of Phe10 indicate that there are very large differences in the flexibility and internal mobility of the protein in response to binding of calcium ions.[27,28] Correspondingly, the changes in the dynamics of the protein in response to calcium binding are currently under investigation by quantitative measurements of amide proton exchange rates and ^{15}N and ^{13}C relaxation. On the basis of the apparent discrepancies between the rather substantial changes in chemical shifts and protein dynamics, yet rather subtle changes in structure upon binding of Ca^{2+}, it became apparent that very high quality, high-resolution structures would be required to reliably establish the structural differences between the calcium-free and calcium-loaded states of calbindin D_{9k}.

The calculations of high-resolution *fourth generation*[30] solution structures of apo and calcium-loaded calbindin D_{9k} derived by NMR spectroscopy are nearly completed. These have been calculated from ~1000 distance constraints determined from NOEs, ~150 dihedral angle constraints, and 25 hydrogen bond constraints, using an approach that combines distance geometry (DISGEO[31]) and restrained molecular dynamics[32] calculations. The quality of the input constraints for the apo and calcium-loaded states are approximately equal, and we expect that calculated

(19) Wüthrich, K.; Billeter, M.; Braun, W. *J. Mol. Biol.* **1984**, *180*, 715–740.
(20) Chazin, W. J.; Kördel, J.; Drakenberg, T.; Thulin, E.; Brodin, P.; Grundström, T.; Forsén, S. *Proc. Natl. Acad. Sci. U.S.A.* **1989**, *86*, 2195–2198.
(21) Svensson, A.; Thulin, E.; Forsén, S. *J. Mol. Biol.* **1992**, *223*, 601–606.
(22) Drakenberg, T.; Hofmann, T.; Chazin, W. J. *Biochemistry* **1989**, *28*, 5946–5954.
(23) Kördel, J.; Forsén, S.; Chazin, W. J. *Biochemistry* **1989**, *28*, 7065–7074.
(24) Kördel, J.; Forsén, S.; Drakenberg, T.; Chazin, W. J. *Biochemistry* **1990**, *29*, 4400–4409.
(25) Akke, M.; Drakenberg, T.; Chazin, W. J. *Biochemistry* **1992**, *31*, 1011–1020.
(26) Skelton, N. J.; Forsén, S.; Chazin, W. J. *Biochemistry* **1990**, *29*, 5752–5761.
(27) Skelton, N. J.; Kördel, J.; Forsén, S.; Chazin, W. J. *J. Mol. Biol.* **1990**, *213*, 593–598.
(28) Akke, M.; Forsén, S.; Chazin, W. J. *J. Mol. Biol.* **1991**, *220*, 173–189.
(29) Linse, S.; Teleman, O.; Drakenberg, T. *Biochemistry* **1990**, *29*, 5925–5934.
(30) Clore, M.; Gronenborn, A. *Science* **1991**, *252*, 1390–1399.

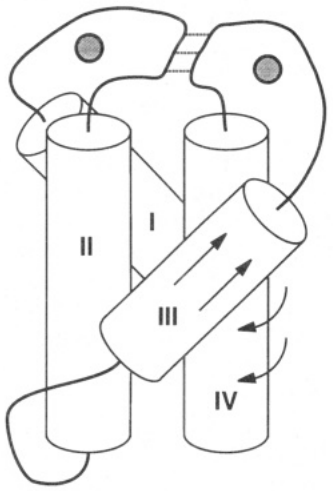

Figure 2. Schematic representation of conformational changes upon Ca^{2+} binding in calbindin D_{9k}.

structures also will be of similar quality. By way of example, the present Ca^{2+}-loaded structures have an average total energy of −1050 kcal·mol^{-1}, constraint energies of <25 kcal·mol^{-1}, average dihedral angle violations of 0.03°, average NOE violations of 0.05 Å, and no NOE violations greater than 0.3 Å. The average RMSD from the average structure is 0.45 Å for the backbone atoms of the four helices.[33] Together these statistics indicate that the structures are of very high quality.

An outline of the structural consequences of the binding of calcium ions was revealed by comparisons of the preliminary solution structures as summarized schematically in Figure 2. Significant perturbations are apparent in the C-terminal EF-hand, including translation of helix III and rotation of helix IV. By contrast, very little effect is observed on the structure of the N-terminal EF-hand. There are no instances where substantial changes in local backbone conformation are observed and all of the helical elements are found in essentially the same locations. This explains why no substantial changes were indicated by our initial analysis of the structural consequences of Ca^{2+} binding, since that analysis was largely limited to the comparison of local geometries and had little information concerning the packing of the major structural elements of the protein. Much larger changes in the conformation upon binding of Ca^{2+} are proposed in the *model* based on the X-ray crystal structure of TnC.[34] However, these differences may be due to either the unusual primary structure of the N-terminal pseudo-EF-hand in calbindin D_{9k} or inherent differences in calcium sensors such as TnC and calcium buffers such as calbindin D_{9k}.[35] A more detailed analysis of the structural consequences of the binding of Ca^{2+} ions in calbindin D_{9k} will be possible once the three-dimensional structures have been fully refined.

(31) Havel, T.; Wüthrich, K. *Bull. Math. Biol.* **1984**, *46*, 674–698.
(32) Scheek, R. M.; Van Gunsteren, W. F.; Kaptein, R. *Methods Enzymol.* **1989**, *177*, 204–218.
(33) Kördel, J.; Skelton, N.; Akke, M.; Chazin, W. J. *J. Mol. Biol.* **1992**, submitted.
(34) Herzberg, O.; Moult, J.; James, M. N. G. *J. Biol. Chem.* **1986**, *261*, 2638–2644.
(35) daSilva, A. C. R.; Reinach, F. C. *Trends Biochem. Sci.* **1991**, *16*, 53–57.

Addressing Cooperativity and the Role of Surface Charges in Calcium Binding

As mentioned in the introduction, cooperativity in the binding of Ca^{2+} ions is observed for many members of the CaM superfamily of proteins, including calbindin D_{9k}. Even a seemingly simple molecular system with only two binding sites becomes nontrivial when site affinities depend on the extent of occupancy.[36] A general scheme is shown in Figure 3 in which macroscopic (K_1 and K_2) and microscopic (K_I, K_{II}, $K_{I,II}$ and $K_{II,I}$) Ca^{2+}-binding constants are defined. The macroscopic binding constants K_1 and K_2 may be determined from the competition experiments while an assessment of the microscopic binding constants can only be made if it is possible to identify an experimental parameter—spectroscopic or other—that discriminates between different molecular species. Thermodynamically, cooperativity in a two-site system (Figure 3) is given by

$$\Delta\Delta G = \Delta G_{I,II} - \Delta G_I = \Delta G_{II,I} - \Delta G_{II} = -RT \ln (K_{I,II}/K_I) = -RT \ln (K_{II,I}/K_{II}) \quad (1)$$

Negative $\Delta\Delta G$ implies positive cooperativity.

(i) Charge Mutations and Experimental Determination of Cooperative Binding. Despite the central role played by electrostatic interaction in proteins, there is still considerable uncertainty regarding the treatment of such interactions by theoretical methods. Furthermore, there are few detailed and systematic experimental studies against which different models and approximations may be tested. Calbindin D_{9k} constitutes a good model system for testing various aspects of charge–charge interactions in proteins as we will show in the following sections.

Inspection of the X-ray structure of bovine calbindin D_{9k}[2] reveals that it has a markedly asymmetric charge distribution. There is an excess of negatively charged amino acids at and around the Ca^{2+}-binding sites. At neutral pH the net charge is −7 for the apo state and −3 for the Ca^{2+}-saturated state. What role does this charge asymmetry play for the functional properties of the protein? In particular, what is the effect on Ca^{2+} binding and the stability toward unfolding? A diagram of the Ca^{2+}-binding sites in the crystal structure of calbindin D_{9k}[2] is shown in Figure 4, indicating the positions of some of the negatively charged surface residues and their distances to the two Ca^{2+} ions. A powerful feature of site-directed mutagenesis is that charges in proteins can be introduced or removed. In the case of calbindin D_{9k} three of the acidic surface residues (Glu17, Asp19, and Glu26) close to—but not coordinating—the two Ca^{2+} ions have been neutralized by substituting them with the corresponding amides. All in all, seven mutants have been prepared comprising all possible single, double, and triple mutants.

The Ca^{2+} affinity of wild-type calbindin D_{9k} and the seven mutants was determined using a binding competition method involving fluorescent and/or chromophoric Ca^{2+} chelators with Ca^{2+} affinities similar to those of the protein (Quin 2, 5,5′-Br_2-BAPTA; cf. ref 37). The experimental values of the macroscopic

(36) Klotz, I. M. Introduction to Biomolecular Energetics; Academic Press: London, 1986; pp 103–133.
(37) Tsien, R. *Biochemistry* **1980**, *19*, 2396–2404.

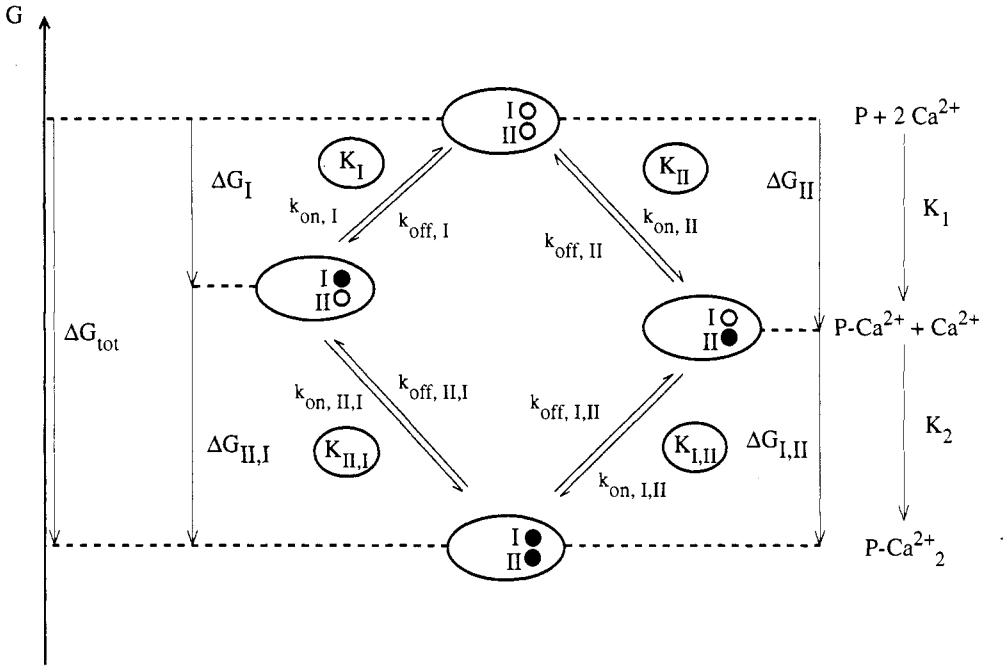

Figure 3. Model for calcium binding to calbindin D_{9k}. Macroscopic (K_1 and K_2) and microscopic (K_I, K_{II}, $K_{I,II}$, and $K_{II,I}$) Ca^{2+} binding constants are defined and free energy changes involved are indicated.

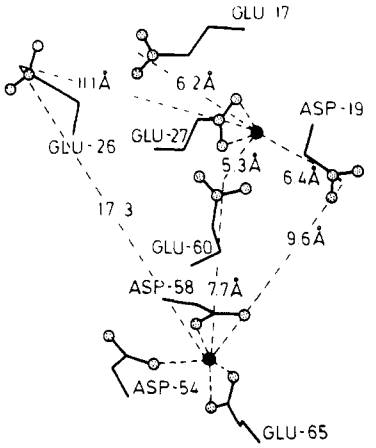

Figure 4. Diagram of the Ca^{2+}-binding sites of calbindin D_{9k} based on the crystal structure.[4] The positions of the negatively charged surface residues in the vicinity of the binding sites are shown, along with relevant distances (in angstroms) to the calcium ions.

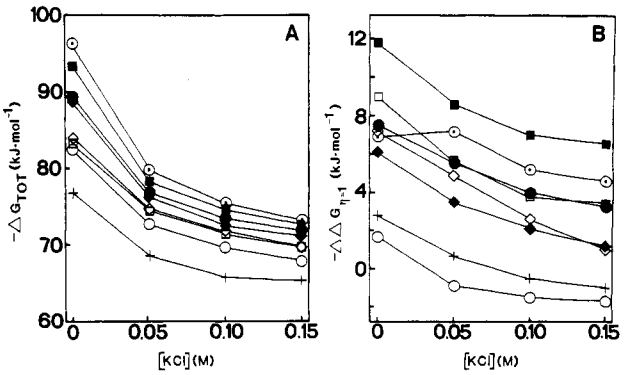

Figure 5. (A) Free energy of binding of two Ca^{2+} ions, ΔG_{tot}, and (B) the lower limit of the free energy of interaction between the two Ca^{2+}-binding sites, $-\Delta\Delta G_{\eta=1}$, as a function of KCl concentration for (⊙) the wild-type protein, (●) E17Q, (◆) D19N, (■) E26Q, (○) (E17Q+D19N), (□) (E17Q+E26Q), (◇) (D19N+E26Q), and (+) (E17Q+D19N+E26Q). Reprinted with permission from ref 38. Copyright 1991 American Chemical Society.

binding constants K_1 and K_2 in moles/liter for the wild-type and seven surface charge mutants at different ionic strengths can be used to calculate the total free energy of binding of two Ca^{2+} ions according to $\Delta G_{tot} = RT \ln (K_1K_2)$. The result is shown in Figure 5A.[38] It is obvious that the negative surface charges, although not directly involved in Ca^{2+} ligation, contribute significantly to the Ca^{2+} affinity. The effect is most pronounced at low ionic strength where on average, each of the studied surface charges contributes −7 kJ/mol to ΔG_{tot}. In the mutant with three surface charges neutralized, the decrease in the product of K_1 and K_2 relative to the wild-type is nearly 10^4-fold. In the presence of KCl the effect of surface charges on the Ca^{2+} affinity is diminished but not eliminated. Not surprisingly the salt effect decreases with number of negative surface charges.

The macroscopic Ca^{2+}-binding constant K_2 is greater than K_1, in the wild-type as well as in most mutants. Clearly the Ca^{2+} binding is a cooperative phenomenon. The expression for $\Delta\Delta G$ (in eq 1) can be rewritten, noting that $K_1 = K_I + K_{II}$ and $K_1K_2 = K_IK_{II,I} = K_{II}K_{I,II}$ as

$$-\Delta\Delta G = RT \ln (4K_2/K_1) + RT \ln ((\eta + 1)^2/4\eta) \quad (2)$$

where $\eta = K_{II}/K_I$. Since the second term in eq 2 has a minimum (equal to zero) for $\eta = 1$, it is possible to determine a lower limit of $-\Delta\Delta G$ solely from the macroscopic binding constants:[39]

$$-\Delta\Delta G_{\eta=1} = RT \ln (4K_2/K_1) \quad (3)$$

The plots of $-\Delta\Delta G_{\eta=1}$ at different ionic strength for the surface charge mutants are shown in Figure 5B.[38] At low ionic strength, wild-type and all mutants show

(38) Linse, S.; Johansson, C.; Brodin, P.; Grundström, T.; Drakenberg, T.; Forsén, S. *Biochemistry* **1991**, *30*, 154–162.

(39) Linse, S.; Brodin, P.; Johansson, C.; Thulin, E.; Grundström, T.; Forsén, S. *Nature* **1988**, *335*, 651–652.

positive cooperativity. The cooperativity seems to become weaker with increasing ionic strength, but it is not completely eliminated at physiological ionic strength except possibly for the mutants (E17Q; D19N) and (E17Q; D19N; E26Q) (remember that $-\Delta\Delta G_{\eta=1}$ is a lower limit of $-\Delta\Delta G$!). By using ^{1}H NMR to monitor the effects of Ca^{2+} titrations, it has been possible to put narrow limits on η for some of the mutant proteins. In the case of the wild-type the best value of η is 1.6 at 50 mM KCl and 1.0 at 150 mM KCl. This corresponds to $-\Delta\Delta G$ values of 7.7 and 4.6 kJ/mol, respectively. These values are close to the $-\Delta\Delta G$ values plotted in Figure 4B; at higher ionic strengths this corresponds to an approximately 8-fold increase in affinity for the second Ca^{2+} ion after binding of the first. For (E17Q; D19N) and (E17Q; D19N; E26Q) η is found to be around 5 at 50 mM KCl; thus $-\Delta\Delta G$ is 0.5 ± 1.7 and 2.1 ± 0.8, respectively. The cooperativity appears to be reduced or eliminated in these two mutants.

These experimental studies represent a unique data set for testing different models for electrostatic interactions in proteins. The observed changes in binding free energy due to changes in surface charges and ionic strength extends over nearly 30 kJ/mol (i.e. more than 5 pK_a units). By comparison pK_a shifts of histidines in proteins due to annihilation of charges are less than 0.5 pK_a unit.[40,41]

(ii) Kinetics of Ca^{2+} Dissociation and Association. Neutralization of surface charges some 6–16 Å away from the Ca^{2+}-binding sites results in a markedly reduced Ca^{2+} affinity. Is this effect due to an increased rate of Ca^{2+} dissociation, to a reduced rate of association, or both? These questions may be answered through kinetic measurements using stopped-flow optical spectroscopy, utilizing the fluorescent chelator Quin 2 to monitor the release of Ca^{2+} from the Ca^{2+}-loaded protein.[42-44] Stopped-flow studies were carried out both at low ionic strength and with 0.1 M KCl added. A summary of observed Ca^{2+} dissociation rates is given in Table I. Four of the mutant proteins show two clearly resolvable kinetic processes at low ionic strength, each of which appears to correspond to the dissociation of a single Ca^{2+} ion, whereas the other four show a single process corresponding to the dissociation of two Ca^{2+} ions. Table I shows that the change in off-rate from the wild-type protein to the triple mutant (E17Q; D19N; E26Q) does not reflect the nearly 2-fold change in each of the macroscopic binding constants. Thus, at this stage, we may already infer that the on-rates must be lowered considerably. The dissociation can be assumed to occur via either the left or right pathway of Figure 3, and this allows us to calculate a maximum rate constant for the binding of Ca^{2+} to site I or site II when the other site is empty. Two extreme cases are possible for the dissociation kinetics:[44] (i) dissociation occurs mainly via the left pathway of Figure 3 with the second Ca^{2+} ion dissociating from site I. Thus $K_1 = k_{I,on}/k_{I,off}$.

(40) Thomas, P. G.; Russell, A. J.; Fersht, A. R. *Nature* **1985**, *318*, 375–376.
(41) Sternberg, J. E.; Hayes, F. R. F.; Russell, A. J.; Thomas, P. G.; Fersht, A. R. *Nature* **1987**, *330*, 86–88.
(42) Martin, S. R.; Andersson-Teleman, A.; Bayley, P. M.; Drakenberg, T.; Forsén, S. *Eur. J. Biochem.* **1985**, *151*, 543–550.
(43) Forsén, S.; Linse, S.; Thulin, E.; Lindegård, B.; Martin, S. R.; Bayley, P. M.; Brodin, P.; Grundström, T. *Eur. J. Biochem.* **1988**, *177*, 47–52.
(44) Martin, S. R.; Linse, S.; Johansson, C.; Bayley, P. M.; Forsén, S. *Biochemistry* **1990**, *29*, 4188–4193.

Table I. Dissociation Rate and Maximum Association Rate Constants for Different Calbindin D_{9k} Mutants at "Low" and "High" Ionic Strength

	k_{off} (s^{-1})[a]		$k_{on,max}$ (M^{-1} s^{-1})	
protein	0 M KCl[b]	0.10 M KCl	0 M KCl	0.10 M KCl
wild-type	3.5	8.6 (48.0)	9×10^8	2×10^7
E17Q	4.3	11.0 (100)	2×10^8	2×10^7
D19N	8.3 (21.5)	12.5 (48.6)	3×10^8	4×10^7
E26Q	2.4 (12.4)	4.9 (69.3)	2×10^8	2×10^7
E17Q; D19N	6.3 (15.3)	8.5 (22.7)	2×10^8	1×10^7
E17Q; E26Q	3.9 (18.3)	8.7 (132)	3×10^7	1×10^7
D19N; E26Q	4.8	3.9 (12.3)	7×10^7	1×10^7
E17Q; D19N; E26Q	3.4	10.7 (370[c])	2×10^7	1×10^7

[a] Values in parentheses refer to an additional fast process if detectable. [b] If counterions and buffer ions are accounted for, the ion concentration might be as high as 25 mM in these measurements; hence low rather than 0 ionic strength. [c] Measured through ^{43}Ca NMR line-shape analysis of ^{43}Ca NMR signals from calbindin D_{9k} solutions containing a slight excess of ^{43}C.[43,44] The rates of Ca^{2+} exchange were evaluated as in ref 59.

However, the maximum value of K_I is equal to K_1 and therefore $k_{I,on}(max) = k_{I,off}K_I$. (ii) For dissociation predominantly via the right pathway we find by analogous reasoning, that $k_{II,on}(max) = k_{II,off}K_I$. Equating the off-rates with the slow dissociation step observed experimentally, we may now calculate values for the maximum association rate constants for binding to either site I or II under conditions where the other is unoccupied (Table I). When only a single exponential dissociation step is observed, the interpretation of the rate data is different but the inferred maximum rate constants only deviate slightly from that given above. Thus, it is evident that charge neutralization has resulted in decreased rate constants for Ca^{2+} binding to the Ca^{2+}-free protein at low ionic strength. If the cluster of negative surface charges on calbindin D_{9k} has a direct influence on the rate of association of Ca^{2+}, one would expect to find a decrease in the association rate at higher ionic strengths. This effect should be most pronounced for the wild-type and least pronounced in the triple mutant with three of the surface charges neutralized for which the net charge of the protein should be zero. In Table I we see that the association rate constant for Ca^{2+} binding is indeed reduced at higher ionic strengths—the effect being very significant for the wild-type but only slight for the triple mutant!

(iii) Thermochemistry of Ca^{2+} Binding. Can the surface charge effects on Ca^{2+} affinity be further characterized in thermodynamic terms? In particular, is the reduced Ca^{2+} affinity associated with decreased negative surface charge due to changes in ΔH, $T\Delta S$, or both? Such a discrete partitioning may be accomplished through calorimetric measurement of the enthalpy of the Ca^{2+}-binding process:

$$2(Ca^{2+})_{aq} + \text{apo-calbindin } D_{9k} \xrightarrow{\Delta H_{tot}} (Ca^{2+})_2\text{–calbindin } D_{9k} + \text{aq} \quad (4)$$

where the subscript aq helps to identify that water of hydration is liberated in the reaction. Needless to say, water of hydration associated with groups on the protein will also become reorganized in the binding process. Microcalorimetric measurements of the enthalpy change upon Ca^{2+} binding to wild-type calbindin D_{9k} and the seven charge neutralization mutants have been carried

out.[45] For all eight proteins, the enthalpy change is nearly linearly dependent on the total amount of Ca^{2+} added up to a Ca^{2+}-to-protein ratio of about 2. From the experimental values of ΔH_{tot} and the known value of $\Delta G_{tot} = -RT \ln (K_1K_2)$, values of $T\delta S_{tot}$ are calculated. The values for the mutants with one or two surface charges neutralized can be averaged since the spread of values within each group is small. Throughout the series of mutant proteins ΔH is small (in the range −15 to −17 kJ/mol) and the observed changes in ΔG_{tot} as successive surface charges are neutralized are consequently not due to changes in enthalpy of binding. We may thus conclude that the changes in ΔG_{tot} are largely the result of changes in the entropy term, $T\delta S_{tot}$![46]

(iv) Toward Determination of the Molecular Basis for Cooperativity. NMR spectroscopy is being applied to study various aspects related to cooperativity in the binding of Ca^{2+} by calbindin D_{9k}. The study of apo and calcium-bound states of the protein offers some insight, but does not provide sufficient information for understanding the molecular basis for cooperativity in the binding of Ca^{2+}. Ideally, studies of the two half-saturated states of the protein are necessary. However, the half-saturated calcium state of the protein is not significantly populated under equilibrium due to the cooperativity of binding; thus it is necessary to modify either the protein or the ion. The objective in this approach is to decrease the affinity of one of the sites so that binding is sequential, while not significantly perturbing the other site. To this end, site-directed mutagenesis is being utilized to alter some of the key side-chain Ca^{2+} ligands. Similar strategies have been utilized to modify the binding affinities to CaM and TnC.[47] A second approach is based on the fact that Cd^{2+} is a good substitute for Ca^{2+}, e.g. ref 48. Cd^{2+} binds to site II of calbindin D_{9k} with normal affinity, but to site I with much lower affinity than Ca^{2+}, which means that half-saturated $(Cd^{2+})_1$–calbindin D_{9k} can be readily prepared.[49] Detailed 2D ^1H NMR studies of $(Cd^{2+})_1$–calbindin D_{9k} have been completed.[28] Initially $(Cd^{2+})_2$–calbindin D_{9k} was compared to the Ca^{2+}-loaded protein, demonstrating that Cd^{2+} represents a viable model for Ca^{2+} when bound to calbindin D_{9k}. Next, virtually complete ^1H NMR assignments were obtained for $(Cd^{2+})_1$–calbindin D_{9k}, and the elements of secondary structure and global folding pattern were identified. Comparisons to the apo and Ca^{2+}-loaded protein show that all three structures are very similar. Although structural consequences are small, the effects on a variety of NMR parameters that reflect the mobility and flexibility of the protein are readily apparent. The changes in the backbone amide proton exchange, aromatic ring flip, backbone, and side-chain scalar coupling constants, and proton chemical shifts, all indicate that the protein becomes increasingly less flexible as Ca^{2+} ions are bound. Furthermore, the studies of the half-saturated protein show that the limited structural effects and the more significant dynamical effects are larger for the binding of the first ion than for the second. Such observations are consistent with the analysis of Cooper and Dryden[50] wherein the "stiffening" of the protein is predicted to be more pronounced for the first binding step, due predominantly to the entropic effect. In summary, these results suggest that the cooperativity in the binding of Ca^{2+} ions by calbindin D_{9k} can be explained by a shift in the protein conformation and dynamics toward the fully loaded state upon binding of the first ion and that entropic effects associated with the protein dynamics appear to play a major role.

(45) Sellers, P. Unpublished.

(46) This finding is in general accordance with the macroscopic electrostatic theory of ion–ion interaction in a temperature-dependent dielectric. Changes in ΔH and $T\Delta S$ for a given change in the electrostatic free energy, ΔG_{el}, are related through $\Delta\Delta H = (\Delta\Delta G_{el}/\epsilon)[d(\epsilon T)/dT]$ and $T\Delta\Delta S = (\Delta\Delta G_{el}/\epsilon)(d\epsilon/dT)$. Consideration of the temperature dependence for water shows that changes in $T\Delta\Delta S$ should be approximately four times the changes in $\Delta\Delta H$.

(47) Putkey, J. A.; Sweeney, H. L.; Campbell, S. T. *J. Biol. Chem.* **1989**, *264*, 12370–12378.

(48) Swain, A. L.; Kretsinger, R. H.; Amma, E. L. *J. Biol. Chem.* **1989**, *264*, 16620–16628.

(49) Vogel, H. J.; Drakenberg, T.; Forsén, S.; O'Neill, J. D. J.; Hofmann, T. *Biochemistry* **1985**, *24*, 3870–3876.

Table II. Free Energy of Unfolding by Urea for Different Calbindin D_{9k} Mutants

calbindin	$\Delta G_{N\rightarrow U}$(5 M) (kJ/mol)[a]	C_m (M)[b]	$\Delta\Delta G_{N\rightarrow U}$(5 M) (kJ/mol)[c]
wild-type	1.2 ± 0.2	5.3	
E17Q	2.8 ± 0.2	5.6	1.6
D19N	4.3 ± 0.3	5.9	3.0
E26Q	1.6 ± 0.2	5.3	0.4
E17Q; D19N	6.2 ± 0.3	6.2	5.0
E17Q; E26Q	2.3 ± 0.2	5.5	1.0
D19N; E26Q	3.4 ± 0.2	5.8	2.2
E17Q; D19N; E26Q	5.1 ± 0.3	6.1	3.8

[a] Free energy of unfolding at 5 M urea. [b] Urea concentration at the transition midpoint. [c] Difference in free energy of unfolding of mutants relative to that of the wild-type protein at 5 M urea.

Surface Charges and Protein Stability toward Unfolding

A detailed understanding of protein folding and stability is one of the most important goals of modern biological research. The surface charge mutants of calbindin D_{9k} offer an opportunity to study the contributions of electrostatic interactions between surface charges to the stability toward unfolding of the protein. The Ca^{2+} loaded state of wild-type calbindin D_{9k} as well as of the seven charge mutants are only marginally unfolded in boiling water or in 8 M urea. The apo states, however, show reversible unfolding under the same conditions. The folding/unfolding process closely matches that expected for a two-state system. In a series of CD experiments, the degree of unfolding by urea of the apo states of the wild-type and seven charge mutants was conveniently followed from the molar ellipticity at 222 nm. The difference in stability between the charge mutants and the wild-type protein was determined both from the extrapolated free energy of unfolding at zero urea concentration (ΔG_0) and from the difference in stability at 5 M urea, $\Delta G_{N\rightarrow U}$ (5 M). Five molar urea is close to the transition midpoint and the use of $\Delta G_{N\rightarrow U}$ (5 M) to assess differences in stability avoids the uncertainties involved in extrapolating to zero urea concentration.[51] In the case of calbindin D_{9k}, the two sets of free energy differences follow the same trend.[52] All seven charge mutants show increased stability relative to the wild-type. Neither the values obtained for the free energy of unfolding at 5 M urea nor the transition midpoint urea concentrations (i.e.

(50) Cooper, A.; Dryden, D. T. F. *Eur. Biophys. J.* **1985**, *11*, 103–109.

(51) Kellis, J. T., Jr.; Nyberg, K.; Sali, D.; Fersht, A. R. *Nature* **1988**, *333*, 784–786.

(52) Akke, M.; Forsén, S. *Proteins* **1990**, *8*, 23–29.

where [N] = [U]) reveal any immediate relationship between the number of charges eliminated and the relative stabilities[52] (cf. Table II).

How can we rationalize the difference in stability of the different mutants? To account for the relative stabilities, we may consider the thermodynamic cycle:

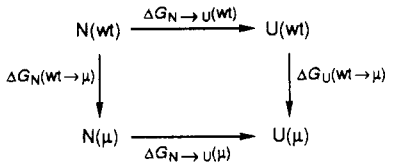

N stands for native, U for unfolded, μ a mutant, and wt the wild-type protein. The experimental quantity $\Delta\Delta G$ (5 M) corresponds to the difference in the free energy of unfolding between the wild-type (wt) and a mutant (μ) and is given by

$$\Delta\Delta G_{N\rightarrow U}(wt\rightarrow\mu) = \Delta G_{N\rightarrow U}(\mu) - \Delta G_{N\rightarrow U}(wt) = \Delta G_{U}(wt\rightarrow\mu) - \Delta G_{N}(wt\rightarrow\mu) \quad (5)$$

If the right-hand quantities are subdivided into contributions due to electrostatic interactions, van der Waals-type interactions, etc., and if we furthermore assume that only electrostatic interactions differ significantly between wild-type and charge mutants, eq 5 can be reduced to

$$\Delta\Delta G_{N\rightarrow U}(wt\rightarrow\mu) = \Delta G_{U,el.stat}(wt\rightarrow\mu) - \Delta G_{N,el.stat}(wt\rightarrow\mu) \quad (6)$$

This implies that the differences in the stability toward unfolding of the wild-type and mutant proteins are predicted to be dependent on the changes in electrostatic free energy for the native and unfolded states. The electrostatic free energies have been calculated using different macroscopic continuum models currently in use in the protein field (for reviews, see refs 53 and 54). Present considerations will be confined to calculations using the Tanford–Kirkwood model for the native state.[55] This model explicitly considers the dielectric boundary between a spherical protein with all charges at the surface and the surrounding solvent. The structure of the folded protein has been assumed to be that of the Ca^{2+}-loaded crystal structure subjected to a 120-ps molecular dynamic simulation in aqueous solution.[56] The unfolded state is probably characterized by a large set of conformations with nearly identical energies and a calculation of the electrostatic free energy is here less straightforward. An extended polypeptide with side chains in staggered conformation has been chosen to represent the unfolded state. Intervals between distant charges have been calculated from the freely-rotating chain statistical mechanical model.[40] Born "self energies" of all surface charges have been assumed to be the same in the unfolded and native states. The electrostatic free energies calculated for the unfolded state are much smaller than those calculated for the native state; thus the difference $\Delta G_N(wt\rightarrow\mu) - \Delta G_U(wt\rightarrow\mu)$ largely reflects changes in the first quantity. The correlation between calculated free energy differences and experimental values of $\Delta\Delta G$ (5 M) is very good (Figure 6)—in particular, the approximate model used reproduces the widely different $\Delta\Delta G_{N\rightarrow U}$ (5 M) within the sets of mutants having the same number of surface charges eliminated. The results clearly show that electrostatic free energies can be an important factor in determining the stability of proteins toward unfolding and that, if increased stability is the goal for some particular application, alteration of surface charges may be an alternative to the introduction of –SS– bonds or other "intraprotein" modifications.

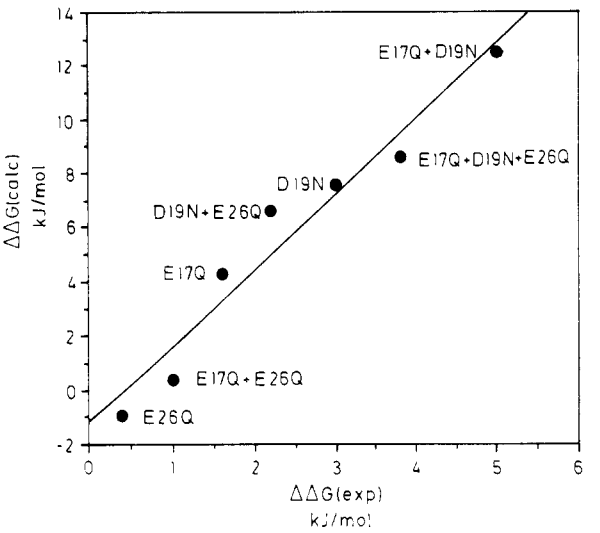

Figure 6. Values of $\Delta\Delta G_{N\rightarrow U}(wt\rightarrow\mu)$ for the Tanford–Kirkwood model[55] compared to the experimental data.

Conclusion and Outlook

Significant inroads have now been made toward understanding the molecular anatomy of calbindin D_{9k} and how this anatomy correlates with various properties of the protein. Calculations of the three-dimensional structure in solution and quantitative measurements of amide proton exchange rates and ^{15}N and ^{13}C relaxation parameters of the apo and calcium-saturated states are now yielding a detailed view of the consequences of calcium binding on the structure and dynamics of the protein. From this high-resolution background it will be possible to extend our biophysical studies and mutagenesis experiments on calbindin D_{9k} in a variety of directions to address issues of primary importance for the EF-hand family of calcium-binding proteins. These include establishing the molecular determinants of ion selectivity, of differences in calcium affinities, and of the cooperativity in calcium binding. These studies will also contribute to the ever-increasing data base of knowledge of protein structure and of the fundamental forces governing protein folding and stability.

We gratefully acknowledge financial support from the Swedish Natural Science Research Council (operating grants to S.F. and graduate as well as postdoctoral fellowship to J.K.) and National Institutes of Health (Grant GM 40120 to W.J.C.).

(53) Harvey, S. C. *Proteins* **1990**, *5*, 78–92.
(54) Sharp, K. A.; Honig, B. *Annu. Rev. Biophys. Biophys. Chem.* **1990**, *19*, 301–332.
(55) Tanford, C.; Kirkwood, J. G. *J. Am. Chem. Soc.* **1957**, *79*, 5333–5339.
(56) Ahlström, P.; Teleman, O.; Kördel, J.; Forsén, S.; Jönsson, B. *Biochemistry* **1989**, *28*, 3205–3211.
(57) Cantor, C. R.; Schimmel, P. R. *Biophysical Chemistry*; Freeman: San Francisco, 1980; Vol. III, p 992.
(58) Kraulis, P. *J. Appl. Crystallogr.* **1991**, *24*, 946–950.
(59) Drakenberg, T.; Forsén, S.; Lilja, H. *J. Magn. Reson.* **1983**, *53*, 412–422.